

STANDARDIZATION OF METHODS FOR EXTRACTING  
STATISTICS FROM SURFACE PROFILE MEASUREMENTS\*

\* \* \*

Peter Z. Takacs  
Brookhaven National Laboratory  
Upton, NY 11973

July, 2014

\*This manuscript has been authored by Brookhaven Science Associates, LLC under Contract No. DE-AC02-98CH10886 with the U.S. Department of Energy. The United States Government retains, and the publisher, by accepting the article for publication, acknowledges, a world-wide licence to publish or reproduce the published form of this manuscript, or allow others to do so, for the United States Government purposes.

## DISCLAIMER

*\*This work was prepared as an account of work sponsored by an agency of the United States Government. Neither the United States Government nor any agency thereof, nor any of their employees, nor any of their contractors, subcontractors, or their employees, makes any warranty, express or implied, or assumes any legal liability or responsibility for the accuracy, completeness, or any third party's use or the results of such use of any information, apparatus, product, or process disclosed, or represents that its use would not infringe privately owned rights. Reference herein to any specific commercial product, process, or service by trade name, trademark, manufacturer, or otherwise, does not necessarily constitute or imply its endorsement, recommendation, or favoring by the United States Government or any agency thereof or its contractors or subcontractors. The views and opinions of authors expressed herein do not necessarily state or reflect those of the United States Government or any agency thereof.*

# Standardization of methods for extracting statistics from surface profile measurements

Peter Z. Takacs

Department of Energy, Office of Basic Energy Sciences  
Brookhaven National Laboratory, Instrumentation Division 535B, Upton, NY 11973

## ABSTRACT

Surface profilers and optical interferometers produce 2D maps of surface and wavefront topography. Traditional standards and methods for characterizing the properties of these surfaces use coordinate space representations of the surface topography. The computing power available today in modest personal computers makes it easy to transform into frequency space and apply well-known signal processing techniques to analyze the data. The Power Spectral Density (PSD) function of the surface height distribution is a powerful tool to assess the quality and characteristics of the surface in question. In order to extract useful information about the spectral distribution of surface roughness or mid-spatial frequency error over a particular spatial frequency band, it is necessary to pre-process the data by first detrending the raw data and then applying a window function before computing the PSD. This process eliminates discontinuities at the borders of the profile that would otherwise produce large amounts of spurious power that would mask the true nature of the surface roughness. This procedure is now part of a new draft standard that is being adopted by the US OEOSC for analysis of the statistics of optical surface, OP1.005.<sup>1</sup> Illustrations of the usefulness of these procedures will be presented.

**Keywords:** Profilometry, surface statistics, PSD, standards, detrending

## 1. INTRODUCTION

Surface finish is an important consideration in the manufacture of high-performance optical components, intimately connected to the magnitude and angular distribution of scattered light from the surface.<sup>2</sup> Sub-nanometer roughness over lateral scales from nanometers to meters affects the performance of optical systems over a wide range of optical wavelengths, from infrared to x-rays. Historically, surface roughness has been characterized by stylus-based surface profiling instruments<sup>3</sup> such as the Talysurf and Talystep machines by Rank Taylor Hobson and the Dektak by Sloan dating from the 1930's. These were analog recording machines providing output on a strip chart recorder. With the advent of digital electronics in the latter decades of the 20<sup>th</sup> century, analog electronics gave way to digital recording capable of orders of magnitude faster data collection and analysis. Phase-measuring interferometers and optical profilers now are commonplace in the optical shop. The computing power of modern microprocessors enables almost instantaneous calculation of the Fourier transform of large 2D data arrays, which has allowed one to easily move from the spatial domain into the frequency domain for analyzing surface properties. The Fourier transform enables calculation of the power spectral density (PSD) of the surface roughness, which is directly related to the angle-resolved scattering of light from smooth surfaces<sup>4</sup>.

Standards for computing surface roughness parameters have been slow to incorporate frequency-domain signal processing techniques. The ASME B46.1-2009 Surface Texture standard<sup>5</sup> and its ISO equivalent, ISO 4287,<sup>6</sup> have evolved over the years to encompass stylus-based profile measurements necessary for characterizing machined surfaces which are inherently rougher than optically-polished surfaces. Analysis is done exclusively in the spatial domain. The optical community uses a very small subset of the parameters defined in B46, primarily the root-mean-square profile roughness, Rq, and the areal roughness, Sq. Additionally, these quantities need to be known over specific spatial frequency bandwidths, which is difficult to do in the spatial domain. Only in the recent B46.1-2009 standard have expressions for sampled data and PSD calculation been added. However, the signal processing steps necessary to condition the data in order not to distort the intrinsic surface PSD have not been addressed. The various RC and Gaussian cut-off filters are defined as complicated function in coordinate space. The ANSI-accredited ASC OP standards committee administered by the Optics and Electro-Optics Standards Council (OEOSC) is developing a standard for extracting statistical information about surface and wavefront errors from sampled profile and areal data with an emphasis on analysis in the spatial frequency domain. OP1.005 – Statistical Evaluation of Optical Surfaces<sup>1</sup> – addresses the need to precisely define all of the factors that enter into the calculation of statistical quantities from sampled digital surface and wavefront data. The following sections are a synopsis of the main points in the standards document.

## 2. BASIC PROFILE MEASUREMENT CONCEPTS

Surface profiling instruments historically began by providing height measurements over a single linear stylus trace along a surface. Most surface texture standards have historically dealt mainly with analyzing linear profile data. Currently available optical profilers and phase measuring interferometers provide height information over a 2D area on the surface. In many cases, these data can be considered to be a series of linear profile measurements and can be treated accordingly. This section addresses concepts used in analyzing 1D linear profile measurements.

### 2.1 Power Spectral Density

The Power Spectral Density (PSD) of a set of  $N$  sampled profile data points,  $Z(x_n)$ , is given by the square magnitude of the Discrete Fourier Transform (DFT) of the detrended and windowed data, where the brute-force definition of the DFT is used here:

$$PSD(p) = \frac{2d}{N} \left| \sum_{n=1}^N e^{i2\pi \frac{(n-1)(p-1)}{N}} \bar{Z}(n)W(n) \right|^2 K(p) \quad (1)$$

where  $\bar{Z}(n)$  is the detrended profile data,  $W(n)$  is the window function, and  $K(p)$  is a book-keeping factor that modifies the first (DC) term and the last term in the DFT to insure that Parseval's theorem holds rigorously for unwindowed data and over the ensemble average:

$$\left\langle \frac{1}{N} \sum_n \bar{Z}_n^2 \right\rangle = \left\langle \frac{1}{Nd} \sum_p PSD_p \right\rangle \quad (2)$$

Note that this is the “one-sided” PSD where  $p$  is a positive integer index and the negative frequencies have been effectively folded into the corresponding positive frequencies. The factor of 2 in the numerator of (1) accounts for this folding, but to avoid double-counting of the DC term at  $p=1$ ,  $K(1) = 1/2$  and, when  $N$  is an even number,  $K((N+2)/2) = 1/2$ . All other values of  $K$  are 1. Also note that the normalization factor for the PSD is the inverse of the total trace length,  $L=Nd$ . See Briggs and Henson<sup>7</sup> for an excellent detailed discussion about the properties of the DFT.

Most numerical analysis programs provide a canned numerical version of the DFT optimized for speed of calculation on a particular system. One must be aware that there is no single convention for normalization of the DFT. The normalization factors are chosen so that applying the forward and inverse DFT to a function will exactly reproduce the original function. But in computing the PSD, one needs to be sure the normalization factor in the forward transform direction is such that Parseval's theorem is exactly satisfied as shown in eqn (2). This expression serves as a check that the correct normalization of the DFT has been used.

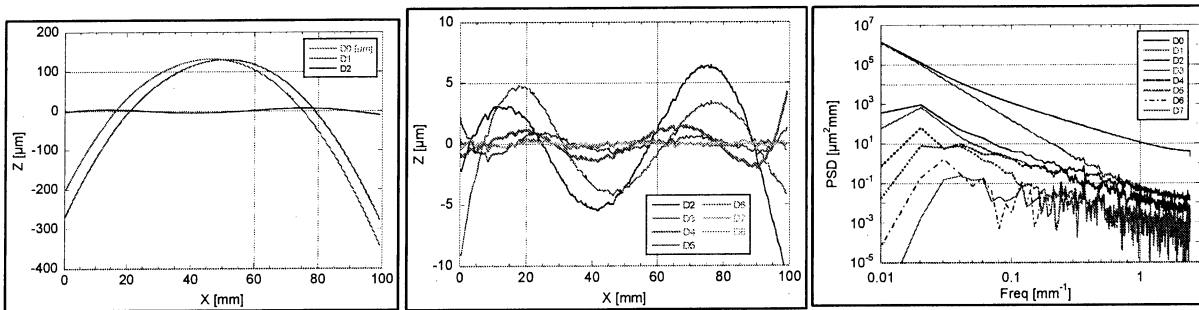


Figure 1 - Effect of detrending on the PSD computed from a surface with significant figure terms. Left two frames show residual profiles after removing the mean (D0) up to an 8th (D8) order polynomial. The corresponding PSD curves are shown on the right. Note the scale change between the 2 profile frames.

### 2.2 Detrending

Detrending the raw data removes low-order figure terms from the profile in order to reduce high-frequency artifacts introduced into the PSD by discontinuities at the endpoints of the profile. Surface profiles with large tilt or curvature need to be flattened, or “pre-whitened”, by removing these low-order polynomial terms<sup>8</sup>. This can be achieved by

least-squares fitting to simple polynomials or to other polynomial functions, such as Chebyshev or Legendre polynomials. For simple linear polynomials, the detrended profile is defined by:

$$\bar{Z}(x_n) = Z(x_n) - [a + bx_n + cx_n^2 + \dots] \quad (3)$$

where  $Z(x_n)$  is the raw data, and the coefficients are computed by simple least-squares fit to the data points. This simple polynomial removes piston (D0), tilt (D1), and curvature (D2), which is usually sufficient for most well-behaved data.

Only when the data has been detrended sufficiently will the intrinsic roughness spectrum emerge from the PSD calculation. The effect of detrending on a float glass surface is shown in Fig. 1. This surface has a particularly large amount of low frequency figure content. The PSD amplitude drops significantly after the curvature is removed (D2), but there is still a large amount of high frequency power in the residuals owing to the discontinuities at the ends of the profiles as seen in the middle frame. Only after the 4<sup>th</sup> order fit is removed do the PSD curves stabilize at high frequency.

### 2.3 Windowing

Another technique useful in extracting the intrinsic spectral character from random roughness profiles is to apply a window function to the finite-length data set.<sup>9</sup> For a window function to be useful in estimating statistics of surface roughness, it should taper smoothly to zero at each endpoint and it must be mean-square normalized to unity<sup>10</sup>:

$$\frac{1}{N} \sum_{n=1}^N W^2(n) = 1 \quad (4)$$

A typical normalized window function that we find useful is the Blackman window:

$$W(n) = \sqrt{\frac{2}{1523}} \left[ 21 - 25 \cos\left(\frac{2\pi(n-1)}{N}\right) + 4 \cos\left(\frac{4\pi(n-1)}{N}\right) \right] \quad (5)$$

Although multiplication of a profile by this function distorts the appearance of the profile, the ensemble average over all profiles does not distort the statistical properties of the data. The following equality holds over the ensemble average, although it does not hold exactly in general for any given profile:

$$\left\langle \sum_n \bar{Z}(n)^2 \right\rangle = \left\langle \sum_n (\bar{Z}(n)W(n))^2 \right\rangle \quad (6)$$

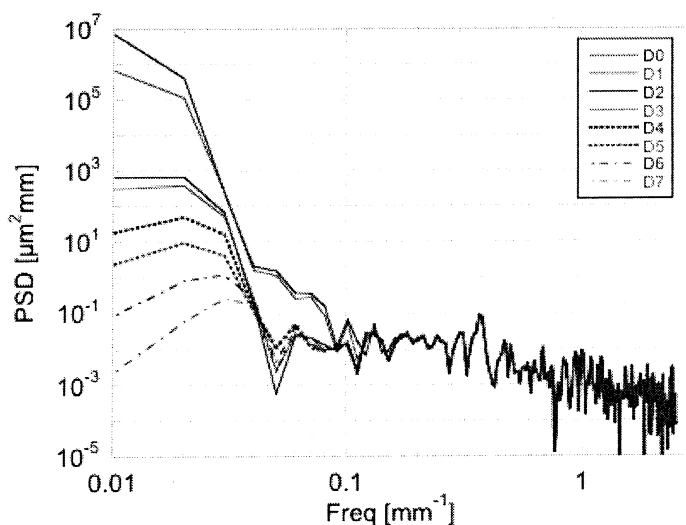


Figure 2 - PSD for profiles in Fig. 1 with Blackman window applied. after detrending. One sees the rapid convergence to a stable PSD after only the first 3 detrending orders are applied - piston, tilt, and curvature.

When the Blackman window is applied to each of the detrended profiles in Fig. 1, the resulting PSD curves are shown in Fig. 2. One can see immediately from these PSD curves that the windowing removes essentially all of the low-frequency power that leaks to higher frequencies, even for the low order detrended profiles that have significant edge discontinuities. All of the PSD curves quickly stabilize to the intrinsic roughness PSD after the first few low frequency harmonics. If one is only interested in the statistics at spatial frequencies beyond the first decade, then it is not even necessary to remove any of the low-order figure terms from the profile, but in practice it is best to at least remove the curvature term before windowing.

One problem with the use of the periodogram as an estimator for the profile PSD is that it is not a consistent estimator – its variance does not decrease as the number of samples increases. There are large fluctuations between adjacent frequency components in the PSD, analogous to speckle in reflected laser light. Various signal processing methods have been devised to reduce the observed speckle. The most straight forward is to compute the PSD for a series of profile measurements made at different locations on the surface. These could be successive rows in a 2D surface measurement, where each row is treated as a separate linear profile. Each profile is first conditioned by detrending and windowing before tossing it into the PSD calculation. The resultant individual PSD curves are then averaged together to generate a “smoothed” estimate of the underlying surface roughness PSD curve. The variance in the average PSD is reduced by a factor of  $1/N$  where  $N$  is the number of spectra that are averaged.

### 3. AREAL STATISTICS CONSIDERATIONS

Analysis methods in the previous section are based on 1D line-profile measurements. Most optical profilers and interferometers today provide 2D areal maps of surface topography. A few decades ago, computing the 2D Fourier transform of large 2D arrays required significant computer time and resources. Now, large 1K x 1K data arrays can be transformed almost instantaneously with a modest laptop computer. It is only natural to extend the 1D signal processing concepts into the areal domain. Detrending is accomplished by least-squares fitting a 2D surface to the data. Usually this is a low-order polynomial in variables  $x$  and  $y$  or Zernike functions, which remove the major deterministic components from the surface - piston, tilt, and curvature – and other higher-order deterministic features, such as astigmatism and trefoil, that are readily seen in the unprocessed raw surface map. What remains after these deterministic terms are subtracted is the residual surface irregularity and system noise. The residual surface can then be Fourier transformed to produce an areal PSD, APSD, after an appropriate window function is applied, from which the intrinsic surface roughness statistics can be computed.

#### 3.1 Handling of Outlier Points

However, one must be careful in computing the APSD that outlier data points are excluded from the calculation, which is also true in computing 1D PSDs from profile data, but are more difficult to see in the surface maps. Outlier points, such as missing data and spikes, cause havoc with the PSD calculation and must be dealt with beforehand. One way deal with missing data points is shown in Fig. 3 for a wavefront measured by a Fizeau interferometer. One notices in the figure that the circular aperture does not fill the camera array completely, resulting in missing data points outside the valid data region. One cannot blindly use the entire data array in the DFT calculation, otherwise it will fail to compute sensible numbers. There are also other artifacts that appear in this data set, such as missing points in the center and near location (550, 275), that need to be avoided. One way to deal with isolated missing points is by interpolating from nearby points to fill in the gap. Some bad data regions are too big to interpolate over without affecting the statistics, such as the region in the center, so these must be excluded from the computation. This is accomplished by defining smaller Regions of Interest (ROIs) within the valid data that exclude the points in question. Three ROIs are shown in Fig 3 as the yellow rectangular regions.

The APSD for the region below center is shown in Fig. 4 with and without a 2D Blackman window applied. The 2D window function is also square normalized to unity so as not to distort the statistics. In this case it is simply the product of two normalized 1D Blackman functions for  $M$  and  $N$  points, where  $M$  and  $N$  are the dimensions of the data array. One can see from the APSD frames on the right side of Fig. 4 that the window function completely suppresses the “diffraction spikes” caused by the discontinuities along the edges of the region extracted from the larger data set. The window function does an excellent job at making the mid and high spatial frequency features visible.

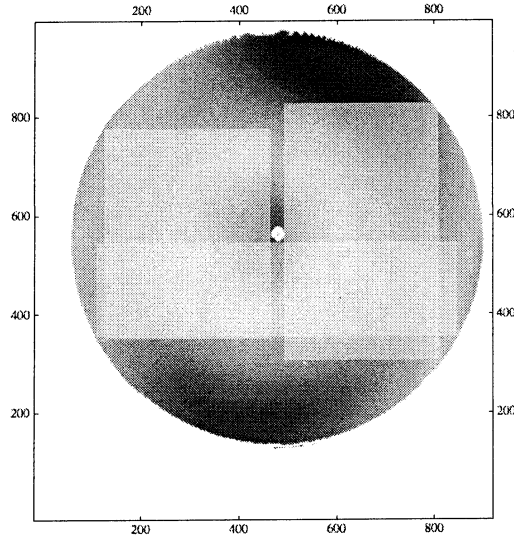


Figure 3 - Residual wavefront map after subtracting piston, tilt, and curvature from a Fizeau interferogram. Three ROIs are shown that exclude missing or bad data points.

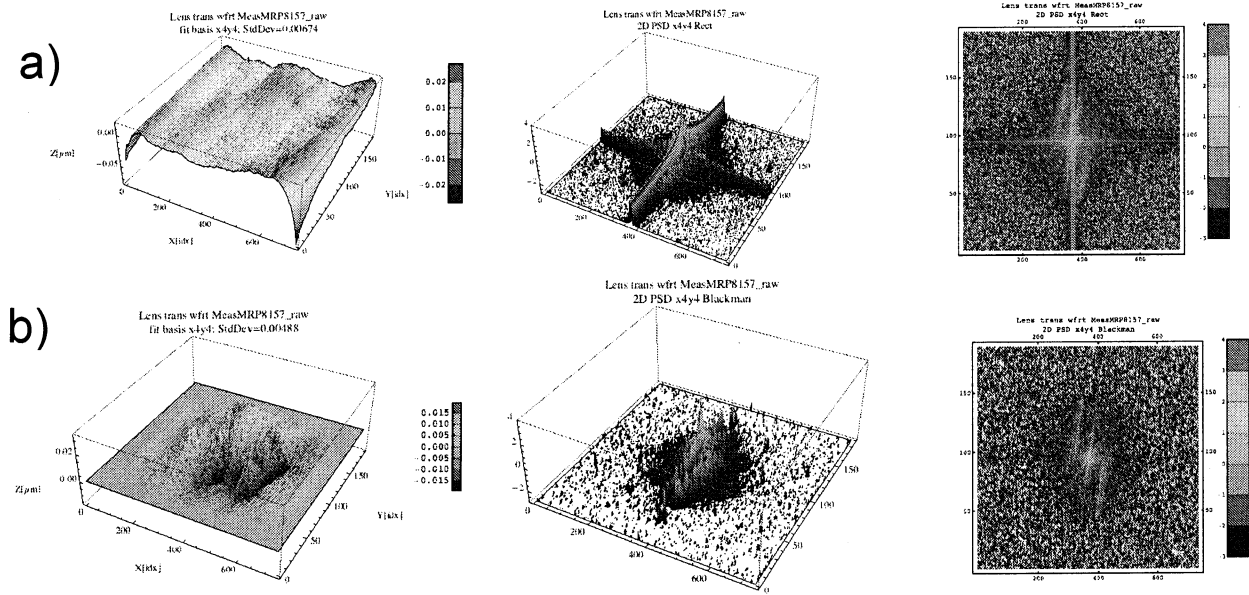


Figure 4 - APSDs computed for the ROI below the center in Fig. 3, where a) is with no window function applied, and b) is with a 2D Blackman window applied. The left frame is the surface ROI with and without the window function applied. The center and right frames are the APSDs in Cartesian coordinates.

### 3.2 PSD considerations in 2D - Areal PSD: APSD

The APSD is always computed in Cartesian frequency space coordinates by a 2D DFT. In many cases, where the residual roughness is isotropic, one would like to convert from a Cartesian space into a radial-azimuthal space and average over all azimuthal angles to end up with a single radial PSD curve (rPSD) that describes the distribution of roughness as a function of radial spatial frequency. This function is useful for computing statistics over specified spatial frequency bandwidths. The practical method for computing the rPSD from the APSD involves binning the points within finite-width radial frequency bands starting at the center of the areal PSD, which is the DC element, and computing the average in each frequency increment band. Although the APSD for the surface ROI shown in Fig. 4 appears to have some low-level directionality, we assume that it is isotropic “enough” and then can collapse the 2D APSD into a single rPSD curve, as shown in Fig. 5. The rPSDs for all 3 ROIs are shown in Fig. 5, along with the mean of all 3. The apparent pixel size for the camera used to record the data determines the Nyquist frequency in

the observed rPSD and is a function of the system zoom magnification. For the present data set, the projected pixel size is  $58.7 \mu\text{m}$ , which gives a Nyquist frequency of  $f_{\text{Ny}} = 1/(2 \cdot \text{pix}) = 1/(2 \cdot 58.7) = 0.0085 \mu\text{m}^{-1}$  along one axis. The highest frequency component in the rPSD is  $0.0120 \mu\text{m}^{-1}$ , which corresponds to the radial distance from the center to the corners in the APSD plot. This is precisely  $\sqrt{2}$  times the Nyquist frequency along one axis. The steep decline in the rPSD at  $0.0047 \mu\text{m}^{-1}$  corresponding to a distance of  $212 \mu\text{m}$  is probably due to an internal aperture in the interferometer that acts as a spatial filter to block stray light and improve the signal-to-noise ratio at low spatial frequencies. This feature is not readily apparent in the areal plots in Fig. 4. It shows that the practical limit of spatial frequency information occurs away from the Nyquist frequency by a factor of 2.

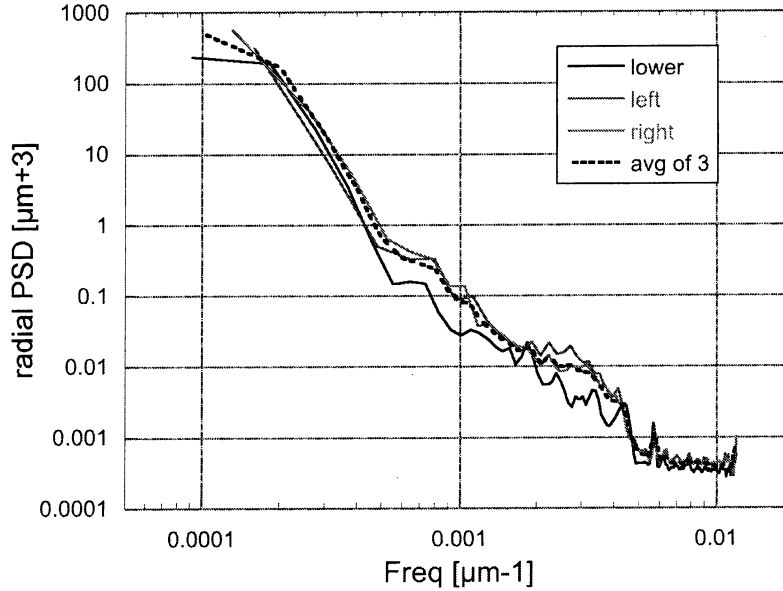


Figure 5 - Radial rPSDs and the mean computed from the APSDs for each of the ROIs in Fig. 3 with a Blackman window applied.

#### 4. BANDWIDTH-LIMITED STATISTICS

After the raw profile input data has been properly conditioned and the PSD has been computed, it is an easy matter to compute statistics from the spectrum. One often needs to specify the RMS roughness,  $R_q$ , over a specific spatial frequency range when using the checkmark indication for surface texture in compliance with ISO 10110-Part 8: Surface Texture. For profile spectra, the  $R_q$  value is given by a sum over the various frequency elements within the specified bandwidth:

$$R_q[f_{lo}, f_{hi}] = \sqrt{f_{\min} \sum_{f=f_{lo}}^{f_{hi}} PSD(f)} \quad (7)$$

where  $f_{\min} = 1/L$  is the lowest frequency component in the computed spectrum, also known as the fundamental frequency. Note that  $f_{\min}$  is the inverse of the total trace length in the ROI.

#### 5. SPATIAL DOMAIN FREQUENCY FILTERING

The previous section gives a simple formula for computing the bandwidth-limited RMS roughness statistic,  $R_q$ , after transforming from the spatial domain into the frequency domain. In some cases, it may be necessary to compute other statistical quantities in the spatial domain from the surface profile directly, quantities that are not derived from the PSD curve. In this case, it is necessary to use the filtered surface profile directly in the calculation. The spatial frequency bandwidth limits are incorporated into the surface profile by applying a Fourier filter to the transformed profile and then inverse transforming back into coordinate space.

Figure 6 shows a simulated random surface profile consisting of 500 points with a sample period of  $d = 1 \mu\text{m}$  and  $R_q = 1 \text{nm}$ . The profile has been detrended to remove piston and tilt. The fundamental frequency for this profile is

$1/500\mu\text{m} = 0.002\mu\text{m}^{-1}$ . All frequency components in the spectrum are integer multiples of this frequency. The frame on the right shows the approximately  $1/f^2$  spectral shape for this 1<sup>st</sup> order autoregressive simulated rough surface.

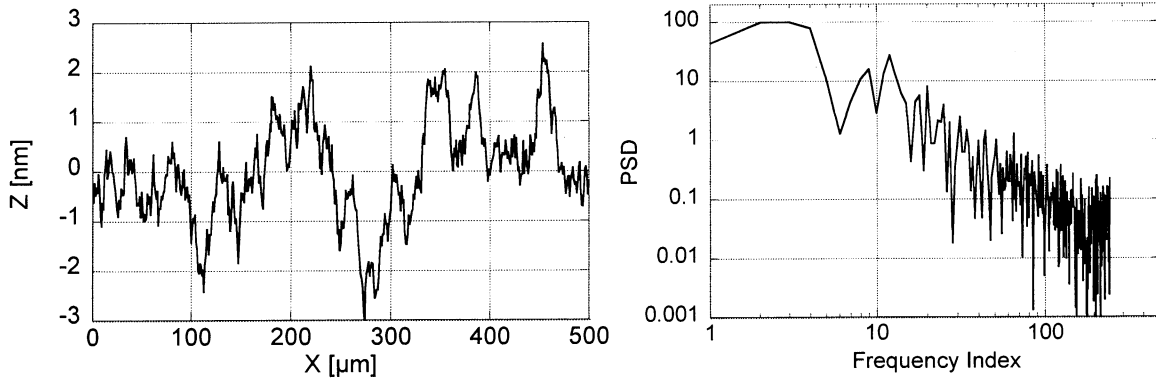


Figure 6 - Simulated random rough profile using order 1 autoregressive series with nominal  $R_q=1\text{nm}$ . Detrending removes piston and tilt, eliminating edge discontinuities. The PSD exhibits the expected inverse-square spectral shape.

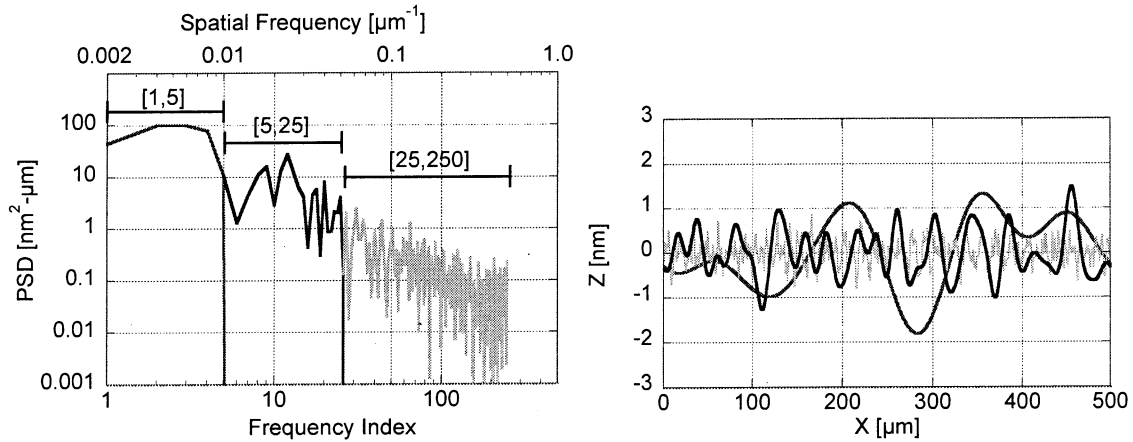


Figure 7 - (Left) PSD of each filtered range, showing the effect of each binary gate frequency filter. (Right) Inverse DFT of the filtered DFT for each profile. Adding all components exactly reproduces the original profile.

When the profile is well-conditioned, as above, it is possible to filter the profile in frequency space by applying a binary gate function to the DFT of the profile and then inverse transforming back into coordinate space. This is illustrated in Figure 7, where simple binary gate functions are applied to the DFT of the profile in Fig. 6 over three adjacent frequency ranges and then the result is inverse transformed to produce the filtered profiles shown on the right. The filter ranges are shown as index numbers that cover the low, mid, and high frequency ranges for this profile. Note that there is no standard to define the boundary between these various spatial frequency ranges. The division is arbitrary and depends mainly on the function of the surface in the optical system.

Table 1 -  $R_q$  values computed for each of the spatial frequency regions shown in Fig. 7.

Freq index range	[1,250]	[1,5]	[5,25]	[25,250]
Freq range $[\mu\text{m}^{-1}]$	[0.002,0.5]	[0.002,0.01]	[0.01,0.05]	[0.05,0.5]
$R_q[f_{lo},f_{hi}]$ [nm]	1.00	0.816	0.526	0.278

The  $R_q$  values for each of the spatial frequency ranges are shown in Table 1. Note that the RSS of the 3 subranges is slightly more than the nominal  $1\text{nm}$  value owing to the overlap of the endpoints of each range. These results indicate that the hard-edge binary gate filter works well to separate the various frequency ranges, provided that the initial profile is well-conditioned. This means, at the minimum, that it has been detrended sufficiently to minimize

endpoint discontinuities. Once the profiles have been filtered in frequency space and reconstituted in coordinate space, it is then possible to compute other statistical quantities directly from the profiles, such as Ra, Rsk, Rku, etc. as defined in ASME B46.1 and ISO 4287. These other quantities are important for manufactured surfaces but are not used much for characterizing highly-polished optical surfaces.

## 6. CLOSING THOUGHTS

This paper has touched on some of the main points contained in the draft standard OP1.005. Time and space limits what can be discussed here. Other issues addressed in the standard relate to concepts associated with surface slope. The B46 and ISO standards treat surface slope as a derived quantity, derived from a height profile measurement. However, some profiling instruments measure surface slope directly and in the case of x-ray mirrors used at extreme grazing incidence, surface slope may be more important than the height profile for assessing system performance. Surface slope statistics are treated on an equal footing with surface height in OP1.005. However, it must be recognized that surface slope is a vector quantity while height is a scalar function of surface position. To this end, we introduce the symbols  $\vec{G} = G_x \hat{x} + G_y \hat{y}$  to represent the vector gradient as a sum of the two x and y direction components. There is still much yet to do to define standards for slope measurement and how they relate to height.

A final point in the document defines a quasi-random sequence of numbers that can be used to test algorithms devised to compute statistical quantities in any computer code. The number sequence is based upon the well-known Fibonacci sequence that is readily available in most numerical computation packages. The standard number sequence is defined by:

$$Z(i) = \text{Modulo}[\text{Fibonacci}(i), 100] + (i/10)^2 \quad \ni i \in [1, 200] \quad (8)$$

This produces a deterministic set of integers that can be computed exactly whenever needed, rather than having to be copied from a table. The second term adds a parabolic shape to the random part so that the total sequence provides a good test for detrending and windowing as well as PSD calculation. We also set the sampling period for the x-values at  $d = 35 \mu\text{m}$  when the PSD is computed so as to avoid ambiguities that may arise if  $d$  is left to be unity. Tables of mean and Rq values are included for various combinations of detrending and windowing applied to the data set. These numbers should be reproduced exactly by any code devised to compute these functions.

One other open notational issue is the symbol for the power spectral density function. There are a number of symbols that have been used to designate the PSD function:  $W$ ,  $S$ ,  $f$ ,  $p$ ,  $P$ , but each of these symbols already has some other accepted usage. For the present, the PSD is denoted by "PSD" with delimiters to specify particular cases, such as  $\text{PSD}_z$  for profile height,  $\text{PSD}_G$  for profile slope,  $\text{APSD}$  for areal 2D PSD, and  $\text{rPSD}$  for radial PSD.

## ACKNOWLEDGEMENTS

I would like to acknowledge the support and encouragement of the OEOSC OP committee in overseeing the development of the OP1.005 standard. I am especially indebted to Dr. Eugene L. Church, my long-time mentor and collaborator, for providing most of the concepts that have gone into this paper. Any mistakes or inconsistencies are entirely of my own doing.

## DISCLAIMER

This report was prepared as an account of work sponsored by an agency of the United States Government. Neither the United States Government nor any agency thereof, nor any of their employees, nor any of their contractors, subcontractors, or their employees, makes any warranty, express or implied, or assumes any legal liability or responsibility for the accuracy, completeness, or any third party's use or the results of such use of any information, apparatus, product, or process disclosed, or represents that its use would not infringe privately owned rights. Reference herein to any specific commercial product, process, or service by trade name, trademark, manufacturer, or otherwise, does not necessarily constitute or imply its endorsement, recommendation, or favoring by the United States Government or any agency thereof or its contractors or subcontractors. The views and opinions of authors expressed herein do not necessarily state or reflect those of the United States Government or any agency thereof.

## REFERENCES

- [1] ASC OP OEOSC, [OP1.005 - Statistical evaluation of optical surfaces DRAFT], Optics and Electro-Optics Standards Council, Rochester, NY(2014).
- [2] E. L. Church, and P. Z. Takacs, "Chapter 8 - Surface Scattering," in Handbook of Optics, M. Bass, ed., 3rd ed. Geometrical and Physical Optics, Polarized Light, Components and Instruments. , vol. I, McGraw-Hill, (2009).
- [3] H. Dagnall, [Exploring Surface Texture], Rank Taylor Hobson, (1980).
- [4] J. C. Stover, [Optical Scattering: Measurement and Analysis], SPIE Press, (2012).
- [5] ASME, [B46.1-2009 SurfaceTexture (Surface Roughness, Waviness, and Lay)] The American Society of Mechanical Engineers, (2009).
- [6] ISO, [ISO 4287:1997 - Surface texture: Profile method -- Terms, definitions and surface texture parameters], ISO/TC 213, Geneva(1997).
- [7] W. L. Briggs, and V. E. Henson, [The DFT : an owner's manual for the discrete Fourier transform], Society for Industrial and Applied Mathematics, Philadelphia(1995).
- [8] R. B. Blackman, and J. W. Tukey, [The measurement of power spectra, from the point of view of communications engineering], Dover Publications, New York,(1959).
- [9] S. M. Kay, [Modern spectral estimation : theory and application], Prentice Hall, Englewood Cliffs, N.J. (1988).
- [10] E. L. Church, and P. Z. Takacs, "The optimal estimation of finish parameters", in *Optical Scatter: Applications, Measurement, and Theory*, ed. J. C. Stover, Proc. SPIE **1530**, pp. 71-85, (1991)

Notice: This manuscript has been authored by employees of Brookhaven Science Associates, LLC under Contract No. DE-AC02-98CH10886 with the U.S. Department of Energy. The publisher by accepting the manuscript for publication acknowledges that the United States Government retains a non-exclusive, paid-up, irrevocable, world-wide license to publish or reproduce the published form of this manuscript, or allow others to do so, for United States Government purposes.